J Mater Sci (2009) 44:2393–2407
DOI 10.1007/s10853-009-3303-4

Modelling and prediction of the chemical and physical degradation of fibre reinforced plastics

Etienne Kolomoni Ngoy · I. M. D. Campbell · R. G. Reid · R. Paskaramoorthy

Received: 28 November 2008 / Accepted: 26 January 2009 / Published online: 26 February 2009

Abstract Modelling and prediction of the environmental degradation of fibre reinforced plastics (FRP) has been hindered by the complexity of the process. Published works are limited to effects and mechanism characterisation or partial models, most of the time empirical. In this article, an analytical approach is presented which resolves the degradation process into only three components: the chemical link density variation, the cohesion force variation and the stress state modification. The first two are referred to as chemical and physical degradation. Based on material science theories, the analysis demonstrates that in a constant environment an exponential function correlates the chemical and physical degradation to the environmental factors. It is also shown that the chemical and physical degradation rate in a real service environment can be determined in a laboratory in a constant environment based only on the variation of chemical link density. Laboratory experiments show that the model correlates excellently with the degradation process.

Introduction

In their service life, fibre reinforced plastic (FRP) materials face a variety of environmental conditions resulting from natural or artificial factors. These include variable temperature and humidity conditions, energetic radiation, such as ultraviolet (UV) rays from the sun or other artificial sources, and diverse chemical reactants, such as liquid in storage tanks and pipes. These factors are always combined and negatively affect the material properties over the time. The top of a boat, for instance, is subjected to UV rays in combination with corrosive humidity and temperature cycles. The inner surface of a pipe or a storage tank faces wet and corrosive conditions in combination with temperature cycles. The resulting degradation mechanism is complex. Therefore, optimised utilisation of FRP materials requires the availability of a reliable method for quantifying environmental effects and for predicting material lifetimes. This allows for optimal handling of issues related to component design, economic assessment and safety considerations, as well as the technical problems relating to equipment maintenance. In this regard, efforts worldwide are devoted to the modelling of FRP environmental degradation. The high complexity of the process, however, explains why no general model or viable corrosion resistance test method is currently available [1, 2].

In 1994, White and Turnbull [1] presented a comprehensive review of the modelling and prediction issues relating to the environmental degradation of polymers. They underlined the necessity to develop models that allow short-term laboratory data to be used to give an accurate forecast of the lifetime of the component, to assist in material selection and to permit planned economic replacement. Their review, however, noted that no general or accurate model was available at the time. They pointed out that the main difficulty was the great number of chemical and physical processes involved in environmental degradation, and their interactions. A more recent review of the subject by Barkatt [2] in 2001 restated the same conclusion. Barkatt recognised that considerable efforts

E. K. Ngoy (✉) · I. M. D. Campbell · R. G. Reid · R. Paskaramoorthy
DST/NRF Centre of Excellence in Strong Materials and RP/Composites Facility, School of Mechanical, Industrial and Aeronautical Engineering, University of the Witwatersrand, Johannesburg, Private Bag 3. Wits 2050., South Africa
e-mail: ek_yosh@yahoo.fr; Etienne.Ngoy@students.wits.ac.za

had been made to model the degradation of FRP, but unfortunately, no comprehensive models were yet available to provide a quantitative basis for evaluating the performance of FRP. A great number of analyses have been published on the environmental degradation of fibre reinforced plastics. In this regard, four predominant trends have been surveyed in the literature.

The first trend is supported by abundant literature and focuses on the characterisation of effects and/or on the description of mechanisms [1–27]. A large range of material properties has been observed for a wide variety of materials in a number of environments. It has been observed that environmental factors negatively affect the material properties over time. Concerns have arisen regarding the degradation mechanism since this is understood as a prerequisite to any modelling effort.

The second trend in the literature deals with modelling and is also the focus of many published works [1, 10, 26, 28–35]. Modelling efforts, for the most part, are limited to partial models based on a single mechanism dominating the whole process. Such models are mostly based on moisture and/or on temperature effects and are empirical. An example is the model based on hygrothermal stress distributions reported by Springer [10]. This model is based on a three-step method. Firstly, analyses are conducted to determine the temperature and moisture distribution inside the material. Secondly, hygrothermal stresses and strains are calculated based on the distribution of temperature and moisture. In the third step, the change in material performance is evaluated based on the calculated hygrothermal stresses. However, this method is subject to limiting hypotheses, such as that the diffusion should obey Fick's law. A second example is the empirical model based on moisture effects proposed by Prichart et al. [29]. They reported on a case where the kinetic equation was deduced empirically by mathematical regression of experimental data. The changes in tensile strength and modulus of a fibreglass–polyester resin composite were plotted versus the moisture content over the course of an exposure. Two temperatures were used with several fibreglass orientations. It was reported that the predicted behaviour based on that model was good for up to 3 years. Unfortunately, no information on longer time scales is provided. Nakamura et al. [30] suggested an empirical model that allowed for quantification of the combined effect of UV rays, humidity, and cyclic load on the flexural strength of cross-ply laminates of carbon fibre reinforced epoxy.

Another modelling approach is that based on chemical reaction mechanisms especially in the case of hydrolysis and oxidation or photo-oxidation [16, 31–33]. This approach leads to complex mathematical formulae, and parameters in these formulae cannot always be measured. Nevertheless, some analyses attempt to provide a global environmental degradation model. An example is the model proposed by Sevostianov et al. [34] whereby the degradation process is considered to be a progressing damage front that moves through the laminate. The suggested mathematical relation calculates the overall modulus as a function of time arising from the contributions of the modulus of both damaged and undamaged layers. However, this model is affected by several limiting hypotheses and by the omission of the effects of moisture diffusion.

The third trend in the literature goes beyond the characterisation of effects and mechanisms and suggests prediction methods. These methods are based on the assumption that the dominating mechanism is thermally activated and follows the Arrhenius law. The prediction relies on linear extrapolation based on temperature variation. A recent review by Celina [35], however, shows the considerable limitation of this law in many cases. Similarly, studies reported by Prian and Barkatt [26] show the non-applicability of this method in many cases due to supra or sublinear kinetics arising during the degradation process.

Due to the lack of predictive models, some researchers resort to exposure of the FRP material in typical service environments in order to assess the environmental resistance of the material. In this fourth trend, the method requires many years of exposure and tests must be conducted for each climatic area [1, 23]. Similarly, in industry, standards specify the material lifetime based on statistics resulting from many years of practice in the field. This implies that many years of experimentation are required prior to setting the lifetime standard for each new specification. The lack of a reliable method of predicting environmental effects has been a hindrance for extended use of FRP material in fields, such as construction [2, 11, 13] and is a cause of concern in the chemical industry where cases of catastrophic failure due to environmental degradation have been reported [36].

The work presented here suggests an analytical approach based on well established material science laws. The analysis demonstrates that in a constant environment an exponential function correlates the material degradation to the environmental factors. It is also shown that the chemical and physical degradation rates in a real service environment can be determined in a laboratory in a constant environment based only on the variation of the chemical link density. The suggested model is a mathematical function logically derived from material science theories and expresses a qualitative relation between the material degradation and environmental factors.

The method

In order to resolve the complexity of the environmental degradation process, the analysis relies on the fact that,

irrespective of its cause, all environmental degradation results only from one of the following three sub-processes:

(1) Chemical degradation corresponding to the modification of the density of chemical links caused either by chemical attack, thermal attack or UV rays.
(2) Physical degradation corresponding to the deterioration of cohesive forces or plasticization caused by either moisture absorption or temperature increase.
(3) Mechanical degradation corresponding to the modification of the stress state caused by temperature cycles or humidity.

The effects of these three sub-processes are only of two kinds. Firstly, the stiffness matrix is altered. This results from the modification of chemical link density and from the variation of cohesion forces. These effects will be referred to as "chemical and physical degradation". Secondly, the stress state is modified as a result of hygrothermal stresses. The ultimate effect of these two processes is the transformation of the material rheology. Therefore, material rheology provides the common parameter allowing the integration of the two processes into a common mathematical relation which provides the mathematical model. The analysis focuses therefore on the rheological changes in the material.

For the sake of methodology, this article deals only with the chemical and physical degradation. In this first approach, the effects of UV rays will be separated from the remaining chemical degradation factors and will be handled in a different paper because, compared to the remaining chemical degradation factors, UV attack is affected differently by the diffusion process. Cases where environmental factors cause crosslinking (post-cure by UV rays or temperature) or stiffen the material are not seen as degradation. This is because the mechanical strength of the material is not negatively affected. These cases are consequently not considered in the following development.

The method consists of deriving a qualitative mathematical relation between the degradation rate and the environmental factors including the chemical concentration, the moisture, the diffusion coefficient, and the temperature. The qualitative mathematical relation contains theoretical parameters that can be determined experimentally. At first, based on material science theories, the environmental factors are mathematically correlated to the material rheology. Secondly, the chemical and physical degradation is expressed as a function of the material rheology. Then, based on the mathematical relation between the material rheology and the environmental factors, the chemical and physical degradation is expressed as a mathematical function of the environmental factors to derive the mathematical model. The validity of the mathematical model is measured by the degree of correlation between the variation of the degradation index calculated from the model and the variation of the mechanical strength of the material measured experimentally over the course of the degradation.

Additionally, in common practice, the environmental resistance of a composite laminate is guaranteed by a barrier coat, made of a resin rich layer. Thus the barrier coat resistance determines the laminate life expectancy. It is also observed, in general, that the degradation mechanism of FRP initiates in the matrix and affects primarily the matrix based properties [27, 30, 34]. Therefore, the modelling method suggested in this analysis is based on the environmental resistance of the matrix. Though the method can be applied to any thermoset matrix, the experimental analysis is limited to an orthophtalic polyester matrix. The laminate under investigation was designed to be comparable to a standard barrier coat. Exposure of the material corresponds to that of a pipe or storage tank environment without temperature or humidity cycles.

Definitions

As stated in the previous section, alteration of the material stiffness during the chemical and physical degradation is always caused by one of the following two effects:

(1) A chemical effect resulting from the modification of the chemical link density caused either by chemical attack, temperature or UV rays.
(2) A physical effect resulting from the deterioration of cohesive force or plasticization caused by either moisture absorption or temperature variation.

Following the above, indices L_d, C_f and E_d are introduced and are, respectively, the chemical link degradation index, the cohesive force deterioration index, and the stiffness degradation index.

Degradation index of the chemical link density: L_d

It is assumed that for a given material, if the cohesive force is held constant, only the modification of chemical link density determines the degradation. The variation in mechanical properties is then directly related to the variation in chemical link density and thereby the variation in diffusivity. Theoretically, the mechanical resistance of a given material may therefore be expressed as a given critical chemical link density that should assure the material structure will hold against breaking stresses. The index of the degradation of the chemical link density L_d defines the material degradation due only to chemical link breakage and is an increasing value over the course of the degradation.

The chemical link density index L_d is modified only by attack from chemicals, UV rays and temperature, respectively, represented by symbols ch, UV and Th. Mathematically the total variation of L_d is the sum of its variation due to the effects of chemical agents, UV rays and thermal attack, expressed as follows:

$$dL_d = dL_{dch} + dL_{dUV} + dL_{dTh} \quad (1)$$

The term representing the effect of UV rays will now be dropped because this analysis considers only the case where no UV rays are involved. Variation in the rate of L_d is thus obtained by differentiation of Eq. 1 as follows:

$$\frac{dL_d}{dt} = \frac{\partial L_d}{\partial(ch)}\frac{d(ch)}{dt} + \frac{\partial L_d}{\partial(Th)}\frac{d(Th)}{dt} \quad (2)$$

Degradation index of the cohesive force: C_f

For a given material, assuming that the chemical link density is held constant, the degradation is directly related to the decrease of cohesive force and consequently the reduction in the mechanical strength. So, theoretically, the mechanical resistance of a given material may be expressed as a given critical cohesive force level that should assure the material structure will hold against breaking stresses. The cohesive force degradation index defines the material environmental degradation resulting only from the variation of cohesion forces. The index C_f increases when the cohesive force decrease.

The variation of the cohesive force results only from diffused moisture and from temperature variation. On this basis, the degradation rate of the cohesive forces can be mathematically expressed as the sum of only two contributions arising from the variation in the rates of the diffused moisture and temperature:

$$\frac{dC_f}{dt} = \frac{\partial C_f}{\partial(\Delta m)}\frac{d(\Delta m)}{dt} + \frac{\partial C_f}{\partial(Th)}\frac{d(Th)}{dt} \quad (3)$$

where Δm represents the diffused moisture.

The degradation index of the material stiffness: E_d

The index E_d represents the degradation of any material property, such as tensile strength, modulus, etc. The chemical and physical degradation of the material stiffness is the sum of two contributions including chemical link degradation and cohesive force degradation. This can be mathematically expressed as follows:

$$E_d = p_1 L_d + p_2 C_f \quad (4)$$

The factors p_1 and p_2 are weighting factors relating the contribution of the chemical link density and cohesive force to the degree of degradation. The stiffness degradation rate can then be deduced from Eq. 4 by differentiation as follows:

$$\frac{dE_d}{dt} = p_1\frac{dL_d}{dt} + p_2\frac{dC_f}{dt} \quad (5)$$

The next step in this analysis is aimed at the determination of each of the terms in the second part of the Eq. 5. It is intended to express these terms as a function of environmental factors. To this end, the following two sections introduce theoretical assumptions based on material science theories.

Material rheology as a function of chemical link density

It is assumed that the material rheological state is linearly related to a power of the chemical link density. This is mathematically expressed as follows:

$$\left(\frac{1}{\Gamma}\right)_{L_d} = k_1(L_d)^a \quad (6)$$

In Eq. 6, Γ represents a material rheology index, such as the viscosity or stiffness; in which case its inverse expresses the material compliance and a is an empirical positive constant. In the rest of this paper, the symbol k_i represents a positive constant and subscripts following parentheses mean "due to". Thus, Eq. 6 gives the material rheological state due to the degradation state of the chemical link density.

Equation 6 is a logical assumption asserting that the stiffness of a solid polymer is proportional to its chemical link density, or inversely, its material compliance is proportional to the index of chemical link degradation. This means that a specific reduction of the chemical link density results in a corresponding specific reduction of the material stiffness and that the reduction is affected by factors, such as molecular chain length and molecular spatial configuration. This kind of correlation provides the basis of rheometric measures. For instance, in rubber vulcanisation, the crosslink level or molecular weight distribution is linearly related to the shear torque resistance [37]. A similar principle is also used in the equation of Mark-Houwink [38] for the determination of polymer molecular weight in dilute solutions. The study of the melt viscosity of polymers has also established the same kind of correlation between the molecular weight and the polymer melt viscosity. In this case, the exponent of the molecular weight varies from 1.5 to 3.5 [39]. The experimental verification of Eq. 6 for a polyester resin shows that the value of a in Eq. 6 is 1.0 (see Sect. Correlation between the model and experimental results).

Material rheology as a function of environmental factors

Material rheology as a function of moisture content

It is assumed that the material stiffness is inversely proportional to a power of the moisture content and this assumption may be mathematically expressed as follows:

$$\left(\frac{1}{\Delta\Gamma}\right)_{\text{moist}} = k_2\left(\frac{\Delta m}{\rho}\right)^b \tag{7}$$

In this equation Δm is the mass of the diffused moisture measured by the variation in the sample weight over time, ρ is the specific mass of the diffused liquid and b is a positive constant. This assumption results from the consideration that the diffused moisture creates additional separation space between the polymer molecules. The intermolecular distance, r, as well as the dielectric parameter and consequently the intermolecular attraction forces, F_{cf}, are modified. The additional separation space can be expressed as a volume determined by the moisture content as follows:

$$\Delta V = \frac{\Delta m}{\rho} \tag{8}$$

Considering Van der Waal's law for cohesive forces, one can deduce the following equation, and hence Eq. 7′, where b is a positive constant depending on the material:

$$\Delta F_{\text{cf}} = \frac{k_3}{(\Delta r)^d} = \frac{k_4}{(\Delta V)^{d/3}} = k_4\left(\frac{\Delta m}{\rho}\right)^{-d/3} \tag{9}$$

$$\left(\frac{1}{\Delta\Gamma}\right)_{\text{moist}} = \left(\frac{k_5}{\Delta F_{\text{cf}}}\right)_{\text{moist}} = k_6\left(\frac{\Delta m}{\rho}\right)^b \tag{7'}$$

The Eq. 7 assumes that the laminate has been plasticized by the diffused liquid but it can also be applied to the case where the penetrating moisture forms clusters as noted by Marsh et al. [12]. In this case, the resistance to the diffusion process is proportional to the interaction area between the diffused mass and the laminate. This area is equal to the external surface area of the diffused volume and it can also be expressed as a power of the volume.

Material rheology as a function of temperature

It is assumed that the material stiffness is inversely proportional to a power of the temperature variation and this assumption may be mathematically expressed by the following equation, where ΔT is the temperature variation and c is a constant.

$$\left(\frac{1}{\Delta\Gamma}\right)_T = k_7(\Delta T)^c \tag{10}$$

The temperature variation affects the material rheology by modifying the thermal kinetic energy of molecules and consequently the level of segmental motions along with the activation energy for flow. This effect is manifested by variation of the material free volume. Common experimental measurement of this effect shows a linear relation between the temperature and the free volume with a slope change at the glass transition temperature [39, 40]. This can be expressed as follows:

$$\Delta v = k_8\Delta T \tag{11}$$

In this equation Δv is the free volume that can also be expressed in terms of intermolecular radius, r, as shown in Eq. 9. Then Van der Waal's law of cohesive forces can be written in terms of free volume and in terms of temperature as follows:

$$\Delta F_{\text{cf}} = \frac{k_3}{(\Delta r)^d} = \frac{k_9}{(\Delta v)^{d/3}} = \frac{k_{10}}{(\Delta T)^{d/3}} \tag{12}$$

Equation 12 can also be written in terms of material rheology as follows:

$$\left(\frac{k_5}{\Delta F_{\text{cf}}}\right)_T = \left(\frac{1}{\Delta\Gamma}\right)_T = k_{11}(\Delta T)^c \tag{13}$$

where c is a positive constant depending on the material. This equation accounts only for the physical degradation. Chemical degradation including thermolysis and post-curing is already considered in Eq. 6.

Chemical concentration as a function of the material rheology

Let Fig. 1 represents a portion of a pipe or storage tank wall. The wall laminate is exposed to a chemical denoted by ch, and to moisture at a temperature T. l is the laminate thickness. C_0 and C_l are respectively the chemical concentrations at the internal and external surface of the laminate.

According to Fick's law, the concentration C_{ch} is a function of the diffusive rate J which can be expressed as

$$J = -D\frac{\partial C_{\text{ch}}}{\partial l} \tag{14}$$

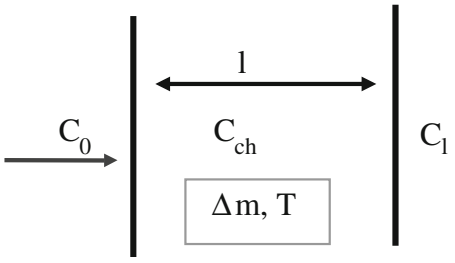

Fig. 1 Portion of pipe wall

where D is the diffusion coefficient. Integration of Eq. 14 (see appendix 1) leads to

$$C_{\mathrm{ch}} = k_{12} D \frac{C_0 - C_l}{l} \tag{15}$$

Since $C_0 \gg C_l$, one can assume that $C_0 - C_l \approx C_0$. Equation 15 can therefore be written as

$$C_{\mathrm{ch}} = k_{12} D \frac{C_0}{l} \tag{16}$$

Analogically to the Stokes-Einstein equation [41, 42], it is assumed that the diffusion coefficient D_0 and the material rheology are related in the following manner:

$$D_0 = k_{13} \frac{T}{\Gamma} \tag{17}$$

where D_0 is the diffusion coefficient at the reference temperature.

Equation 17 represents the effect of material rheology on diffusion and expresses the obvious fact that in a solid material moisture diffusion increases with temperature and decreases with an increase in viscosity. However, the diffusion coefficient is also related to the variation in the thermal kinetic energy of the diffusing molecules according to the Arrhenius law [7, 20, 25] as follows:

$$D = D_0 \mathrm{e}^{\frac{-E_{\mathrm{D}}}{RT}} = k_{13} \frac{T}{\Gamma} \mathrm{e}^{\frac{-E_{\mathrm{D}}}{RT}} \tag{18}$$

In the above equation E_{D} is the activation energy of diffusion. The relation between the concentration C_{ch} and the material rheology is obtained by combining Eqs. 16 and 18:

$$C_{\mathrm{ch}} = k_{14} \frac{T}{\Gamma} \frac{C_0}{l} \mathrm{e}^{\frac{-E_{\mathrm{D}}}{RT}} \tag{19}$$

This relation shows that the concentration of the diffused material inside the laminate depends on its concentration at the laminate surface, on the temperature, on the material viscosity at the given temperature and on the laminate thickness.

However, the material rheology is modified over the course of degradation. The variation of material rheology arises from the variation of chemical link density, L_{d}, and from the variation of cohesion forces due to moisture and temperature. In order to account for this effect, let the total differential of the material rheology be given as a function of these three variables as follows:

$$\mathrm{d}\left(\frac{1}{\Gamma}\right) = \frac{\partial\left(\frac{1}{\Gamma}\right)}{\partial L_{\mathrm{d}}} \mathrm{d}L_{\mathrm{d}} + \frac{\partial\left(\frac{1}{\Gamma}\right)}{\mathrm{d}(\Delta m)} \mathrm{d}(\Delta m) + \frac{\partial\left(\frac{1}{\Gamma}\right)}{\partial T} \mathrm{d}T \tag{20}$$

Integration of Eq. 20 gives the expression of the material rheology as follows:

$$\frac{1}{\Gamma} = \left(\frac{1}{\Gamma}\right)_{L_{\mathrm{d}}} + \left(\frac{1}{\Gamma}\right)_{\mathrm{moist}} + \left(\frac{1}{\Gamma}\right)_{T} \tag{21}$$

Equation 21 is now substituted into Eq. 19. The chemical concentration is then given as a function of the material rheology as follows:

$$C_{\mathrm{ch}} = k_{14} \frac{C_0}{l} \left\{ \left(\frac{T}{\Gamma}\right)_{L_{\mathrm{d}}} + \left(\frac{T}{\Gamma}\right)_{\mathrm{moist}} + \left(\frac{T}{\Gamma}\right)_{T} \right\} \mathrm{e}^{\frac{-E_{\mathrm{D}}}{RT}} \tag{22}$$

Equations 6, 7, 10 and 22 provide relations between the material rheology and environmental factors. These relations provide the basis for combining the effects of these environmental factors into a single mathematical relation. To this end, in the next two sections, the material rheology is related to the degradation rate. The degradation rate is subsequently related to environmental factors, based on the material rheology (Sect. Degradation rate as a function of environmental factors).

Chemical degradation rate as a function of material rheology

Considering again a portion of the pipe wall as represented in Fig. 1, the chemical reaction occurs between the polymeric matrix and the chemical reagent. As the polymeric material constitutes the reaction medium, only the chemical reagent concentration C_{ch} will determine the chemical reaction rate and the law of chemical reaction rates can be expressed as

$$\left(\frac{\partial L_{\mathrm{d}}}{\partial t}\right)_{\mathrm{ch}} = k_{\mathrm{ch}} C_{\mathrm{ch}} \tag{23}$$

In the above equation, k_{ch} is the kinetic constant given by the Arrhenius law.

$$k_{\mathrm{ch}} = A_0 \mathrm{e}^{\frac{-E_{\mathrm{ch}}}{RT}} \tag{24}$$

In Eq. 24, E_{ch} is the activation energy of the chemical reaction, R is the ideal gas constant and A_0 the frequency factor. There are two cases to be considered. Firstly, the reaction at the material surface is not influenced by diffusion and the chemical degradation rate does not depend on the material rheology. According to Eq. 23, the reaction kinetic can be expressed as:

$$\left(\frac{\partial L_{\mathrm{d}}}{\partial t}\right)_{\mathrm{ch}}^{0} = k_{\mathrm{ch}} C_0 \tag{25}$$

where the superscript 0 refers to the laminate surface. Secondly, the reaction inside the laminate where the chemical concentration, and consequently the chemical degradation rate, is a function of the material rheology, which can be obtained by substituting Eq. 22 into Eq. 23:

$$\left(\frac{\partial L_{\mathrm{d}}}{\partial t}\right)_{\mathrm{ch}} = k_{14} k_{\mathrm{ch}} \frac{C_0}{l} \left\{ \left(\frac{T}{\Gamma}\right)_{L_{\mathrm{d}}} + \left(\frac{T}{\Gamma}\right)_{\mathrm{moist}} + \left(\frac{T}{\Gamma}\right)_{T} \right\} \mathrm{e}^{\frac{-E_{\mathrm{D}}}{RT}} \tag{26}$$

From Eq. 2, the chemical link density is also affected by temperature. The temperature effects are of two kinds. A physical effect referred to as thermolysis and a chemical effect referred to as thermal oxidation. The latter is a typical case of an attack by a chemical reagent. Its effects are included in Eq. 26. Thermolysis, however, is an energetic action where bonds are broken by imparting sufficient energy to electrons to pull them out of the bond. The degradation reaction can be schematized as follows:

$$CD + \Delta H_r \rightarrow C + D$$

The rate of reaction is related to the thermal flux in the material [14] as

$$\left(\frac{\partial L_\mathrm{d}}{\partial t}\right)_\mathrm{Th} = \alpha_3 \frac{\Phi_T}{\Delta H_r} \tag{27}$$

In the above equation, Φ_T is the thermal flux, ΔH_r is the thermal energy yield per chain scission and α_3 is a constant. For a given material at constant temperature, the expression $\alpha_3\Phi_T/\Delta H_r$ is a constant. The case where temperature is variable is irrelevant in this analysis as shown later in Sect. The constant environment model.

Thus, from Eqs. 26 and 27, the chemical degradation rate is expressed as function of material rheology as follows:

$$\frac{\partial L_\mathrm{d}}{\partial t} = k_{14}k_\mathrm{ch}\frac{C_0}{l}\left\{\left(\frac{T}{\Gamma}\right)_{L_\mathrm{d}} + \left(\frac{T}{\Gamma}\right)_\mathrm{moist} + \left(\frac{T}{\Gamma}\right)_T\right\} e^{\frac{-E_\mathrm{D}}{RT}} + \alpha_3\frac{\Phi_T}{\Delta H_r} \tag{28}$$

Physical degradation rate as a function of material rheology

This analysis is based on the fact that variation in the material rheology resulting from the change in temperature and moisture is proportional to the cohesive force:

$$F_\mathrm{cf} = k_{15}(\Gamma)_{\mathrm{moist},T} \tag{29}$$

According to the definition given in Sect. Degradation index of the cohesive force: C_f, C_f increases when the cohesive force is reduced. This means that a positive variation in C_f corresponds to a negative variation in the cohesive force as expressed in the following equation:

$$\mathrm{d}C_\mathrm{f} = \mathrm{d}(-F_\mathrm{cf}) = k_{15}\mathrm{d}(-\Gamma) \tag{30}$$

The physical degradation rate as a function of the material rheology is obtained by differentiation of Eq. 30 as follows:

$$\frac{\mathrm{d}C_\mathrm{f}}{\mathrm{d}t} = k_{15}\frac{\mathrm{d}(-\Gamma)}{\mathrm{d}t} = k_{15}\left(\frac{\partial(-\Gamma)}{\partial(\Delta m)}\frac{\mathrm{d}(\Delta m)}{\mathrm{d}t} + \frac{\partial(-\Gamma)}{\partial T}\frac{\mathrm{d}T}{\mathrm{d}t}\right) \tag{31}$$

Degradation rate as a function of environmental factors

Chemical degradation rate as a function of environmental factors

The chemical degradation rate can be expressed as a function of environmental factors by substituting Eqs. 6, 7 and 10 into Eq. 28. This leads to

$$\frac{\mathrm{d}L_\mathrm{d}}{\mathrm{d}t} = \left[\alpha_0 C_0 L_\mathrm{d} + \alpha_1 C_0(\Delta m)^b + \alpha_2 C_0 T^c\right] T\mathrm{e}^{\frac{-(E_\mathrm{ch}+E_\mathrm{D})}{RT}} + \alpha_3\frac{\Phi_T}{\Delta H_r} \tag{32}$$

In the above equation, $\alpha_0 = k_1k_{12}/\mathrm{l}$; $\alpha_1 = k_2k_{12}/\mathrm{l}\rho^b$; and $\alpha_2 = k_7A_0/\mathrm{l}$. These three parameters α_1, α_2, α_3, and generally the symbol α_i in the rest of the paper, are positive constants depending on the material type and environmental conditions. All terms of Eq. 32 are positive and increasing functions of environmental factors. This shows that the chemical degradation rate is an increasing monotonic function of the environment.

Physical degradation rate as a function of environmental factors

In order to determine the physical degradation rate as a function of environmental factors, Eqs. 7 and 10 are substituted into Eq. 30 which gives

$$\frac{\mathrm{d}C_\mathrm{f}}{\mathrm{d}t} = k_{15}\left(\frac{\mathrm{d}(-\Gamma)}{\mathrm{d}t}\right) = k_{15}\left(\frac{\mathrm{d}\left(\frac{\rho}{-\Delta m}\right)^b}{\mathrm{d}t}\right) + k_{15}\left(\frac{\mathrm{d}(-T^{-c})}{\mathrm{d}t}\right) \tag{33}$$

By applying the chain rule of differentiation to the terms on the right side of Eq. 33, one obtains

$$\frac{\mathrm{d}C_\mathrm{f}}{\mathrm{d}t} = \alpha_4\frac{\rho^b}{(\Delta m)^{b+1}}\frac{\mathrm{d}(\Delta m)}{\mathrm{d}t} + \alpha_5\frac{1}{T^{c+1}}\frac{\mathrm{d}T}{\mathrm{d}t} \tag{34}$$

where α_4 and α_5 represent constants.

Chemical and physical degradation rate as a function of environmental factors

The chemical and physical degradation rate of the material is expressed as a function of environmental factors by substituting Eqs. 32 and 34 in Eq. 5.

$$\frac{\mathrm{d}E_\mathrm{d}}{\mathrm{d}t} = \left[\alpha_0 C_0 L_\mathrm{d} + \alpha_1 C_0(\Delta m)^b + \alpha_2 C_0 T^c\right] T\mathrm{e}^{\frac{-(E_\mathrm{ch}+E_\mathrm{D})}{RT}} + \alpha_3\frac{\Phi_T}{\Delta H_r} + \alpha_4\frac{\rho^b}{(\Delta m)^{b+1}}\frac{\mathrm{d}(\Delta m)}{\mathrm{d}t} + \alpha_5\frac{1}{T^{c+1}}\frac{\mathrm{d}T}{\mathrm{d}t} \tag{35}$$

In the above equation, the environmental factors C_0, T and Δm vary with time in a way that is not always

controllable. The exact solution of Eq. 35 requires the determination of the time dependence function of each of the environmental factors. It is not obvious that such a task may be achieved successfully and the solution of the equation would be quite complex. Nevertheless, the problem can be resolved by treating the environmental history as sequence of constant environments as explained in the next section.

The constant environment model

In order to define the method of constant environment, an environmental function defined as below is introduced.

Let f_j be an environmental factor. j is an integer such that $1 \leq j \leq n$. The environmental function, denoted by $\text{env}_t(f_j)$ or env_t, represents an environmental state determined by the values f_j of environmental variables at time t. In addition, the environmental function is such that:

1. $\text{env}_{t2} > \text{env}_{t1}$ only if there exists $q \in [1, n]$ such that for $j = q$, $f_{q2} > f_{q1}$ and $\forall j \neq q$, $f_{j2} \geq f_{j1}$. This means that when the environment changes from state env_{t1} to the state env_{t2}, at least one of the environmental factors increases while all the remaining factors increase or stay constant.
2. env_t is constant only if $\forall j, \Delta f_j = 0$ (all environmental factors are constant).

The environmental factor f_j is a continuous function of time (except for special cases, such as explosion or fire). According to the theorem of mean value for integration, the cumulative effect of f_j over a time interval $\Delta t = t_2 - t_1$, is equivalent to the cumulative effect of a constant value f_{jc} over the same time interval:

$\exists f_{jc} = \text{constant}$, such that $f_j(t_1) < f_{jc} < f_j(t_2)$ and $\int_{t_1}^{t_2} f_j(t)\mathrm{d}t = f_{jc}\Delta t$

This implies that the environmental factor f_j can be represented by a continuous succession of constant values. Therefore, the environment can be modelled as a continuous succession of constant environmental states env_t. The variation of env_t with time can be statistically described by a control chart.

Corollary 1 When env_t = constant, Eq. 35 can be rewritten in a simple form as

$$\frac{\mathrm{d}E_\mathrm{d}}{\mathrm{d}t} = \alpha_0 kTC_0 E_\mathrm{d} + \alpha \tag{36}$$

where k and α are constants defined by the following equations:

$$k = \frac{1}{p_1} \mathrm{e}^{\frac{-(E_\mathrm{D}+E_\mathrm{ch})}{RT}} \tag{37}$$

$$\alpha = \left[\alpha_1 C_0 (\Delta m)^b + \alpha_2 C_0 T^C\right] T \mathrm{e}^{\frac{-(E_\mathrm{ch}+E_\mathrm{D})}{RT}} + \alpha_3 \frac{\Phi_T}{\Delta H_r} + \alpha_4 \frac{\rho^b}{(\Delta m)^{b+1}} \frac{\mathrm{d}(\Delta m)}{\mathrm{d}t} + \alpha_5 \frac{1}{T^{C+1}} \frac{\mathrm{d}T}{\mathrm{d}t} l - T\alpha_0 k C_0 p_2 \left[\alpha_6 \left(\frac{\rho}{\Delta m}\right)^b + \alpha_7 \frac{1}{T^c}\right] \tag{38}$$

Equation 36 was obtained by rewriting Eq. 4 as:

$$L_\mathrm{d} = \frac{1}{p_1}(E_\mathrm{d} - p_2 C_\mathrm{f}) \tag{39}$$

and then by substituting Eq. 39 in Eq. 35, taking into account that env_t is constant.

The rate of change of E_d can be obtained from the solution of Eq. 36. The former is given by the exponential function below, correlating the chemical and physical degradation to time t:

$$\frac{\mathrm{d}E_\mathrm{d}}{\mathrm{d}t} = \alpha \mathrm{e}^{\alpha_0 kTC_0 t} \tag{40}$$

Corollary 2 For env_t = constant, according to Eqs. 5 and 34, the chemical and physical degradation rate of the material stiffness is linearly related to the degradation of the chemical link density as shown below:

$$\frac{\mathrm{d}E_\mathrm{d}}{\mathrm{d}t} = p_1 \frac{\mathrm{d}L_\mathrm{d}}{\mathrm{d}t} \tag{41}$$

This implies that the index L_d is equivalent to index E_d. Practically, this means that in a constant environment, the chemical and physical degradation rate of the material stiffness is determined by the degradation rate of the chemical link density.

Corollary 3 Since the chemical link degradation rate is a monotonic ascending function of the environment (see Sect. Chemical degradation rate as a function of environmental factors), Eq. 41 implies that the degradation rate of the material stiffness is also a monotonic ascending function of the environment:

$$(\text{env}_{t1} \geq \text{env}_{t2}) \Rightarrow \left[\frac{\mathrm{d}E_\mathrm{d}}{\mathrm{d}t}(\text{env}_{t1}) \geq \frac{\mathrm{d}E_\mathrm{d}}{\mathrm{d}t}(\text{env}_{t2})\right] \tag{42}$$

Since the environment is made of a continuous succession of constant environmental states env_t, the chemical and physical degradation rate can be represented by a corresponding succession of exponential functions of the kind represented by Eq. 40. This succession is a monotonic increasing function of env_t.

Prediction method

The above approach provides a method to manage the complexity resulting from the variability of real service

environmental conditions. This constitutes a solution to issues relating to the translatability of laboratory test results to the real service conditions [3].

From all the above, it can be concluded that the real service environmental history can always be determined as a succession of constant environmental states on the basis of the theorem of the mean value:

$$\int_{t_1}^{t_2} f_j(t)\mathrm{d}t = f_{jc}\Delta t \tag{43}$$

Numerical solution of Eq. 43 can always be determined for suitably chosen time intervals. Consequently, the degradation rate history in a real service environment can be exactly determined from laboratory tests conducted in constant environments determined by the real service environmental history. The cumulative degradation over a period can then also be exactly predicted.

Alternatively, the environmental history can be determined as a statistical control chart. Since the degradation rate is a monotonic function of the environmental state, the upper and lower limits on the control chart provide the constant environmental conditions to be used in laboratory to determine the maximum and minimum degradation rates over a period:

$$\frac{\mathrm{d}E_\mathrm{d}}{\mathrm{d}t}\left(\mathrm{env}_{t,\min}\right) \le \frac{\mathrm{d}E_\mathrm{d}}{\mathrm{d}t}\left(\mathrm{env}_{t,\mathrm{real}}\right) \le \frac{\mathrm{d}E_\mathrm{d}}{\mathrm{d}t}\left(\mathrm{env}_{t,\max}\right) \tag{44}$$

In the same way, the average value of the control chart can also be used to determine the average degradation rate over a given period.

Laboratory tests in a constant environment are to be conducted in the following way:

1. The material should be exposed to a constant environment and the constant values of T, C_0, Δm, are provided by the real service environmental history.
2. Following corollary 2, only the change in chemical structure or any other material property linearly related to the material chemical structure needs to be monitored.
3. Then according to corollary 1, the degradation rate function is determined by numerical regression of experimental L_d values using an exponential function.

Discussion

The above analysis has provided a theoretical demonstration of the assertion that, in a constant environment, the chemical and physical degradation of a polymeric material follows an exponential law. Experimental evidence given in Sect. Experimentation provides further validation. The analytical method consists of developing relations between environmental variables and the material lifetime. Theoretical demonstration is also given of the assertion that the physical and chemical degradation rate is a monotonic function of the environment. Consequently, the evaluation of environmental degradation in a laboratory can be conducted in a constant environment and laboratory test results can be directly translated to the real service environment. This provides a solution to issues relating to the transfer of laboratory test results to the real service environment. The prediction method suggested is rigorous and logical consequence of the above assertions.

Experimentation

Experiments were designed in such a way as to simulate storage tank or pipe exposure conditions. The material used was a polyester laminate formulated as presented in Table 1.

Experiment 1

Experimental procedure

Ten sets of five material samples were exposed to a corrosive environment as presented in Table 2. Operating conditions were determined from a table of chemical resistance (Crystic resin) in such a way as to obtain notable degradation in relatively short time.

The experimental procedure was as follows:

1. The samples were initially post-cured for 3 h at 80 °C according to the manufacturer's recommendations for optimal mechanical strength. The samples were then carefully checked for voids or cracks prior to being mounted in the cells of exposure chamber.
2. A fixed volume of 5% sodium hydroxide solution was injected into each cell.
3. All the cells were then immediately mounted on the tray in the exposure chamber where the temperature was already set at 40 °C.
4. Five samples were simultaneously exposed to UV rays, in order to assess the effects of post-curing due to UV rays only. Five others were put into an entirely closed aluminium container which stopped UV rays and the container was then placed in the exposure chamber at the same time in order to determine the post-curing effects due to temperature only.
5. Samples were unloaded one by one from the chamber at 24 h intervals. Unloaded samples were immediately tested for tensile strength and moisture content.

Table 1 Material formulation

	Experiment 1	Experiment 2	Experiment 3
Resin formulation			
Material	Orthophtalic polyester Crystic 196	Orthophtalic polyester NCS 901 PA	Orthophtalic polyester NCS 901 PA
Resin phr	100	100	100
Catalyst phr	2	2	2
Accelerator phr	0.6	–	–
Curing cycle	24 h/25 °C, 3 h/80 °C	24 h/25 °C, 3 h/80 °C	24 h/25 °C, 3 h/80 °C
Laminate			
Composition	Resin/fibre/resin	Res/fib/res/fib/res/fib/res	Res/fib/res/fib/res
Glass fibre	WR 27.4 g/m^2	CSM 300 g/m^2	CSM 300 g/m^2
V_f (%)			
AVG	14	41	14
SD	1.16	1.52	3.1
Thickness (mm)			
AVG	0.21	2.89	2.00
SD	0.02	0.06	–
Void	No voids	No voids	No voids

Table 2 Exposure conditions

Temperature	Constant at 40 °C
UV rays from outside cell	450 μW/cm^2
Humidity from inside cell	100% sample entirely wet
Chemical reagent from inside	5% sodium hydroxide
Maximal duration	10 days

6. All the samples were then scanned using a Raman spectrometer for changes in chemical structure.

Experimental results and discussion

Chemical structure change Raman spectrometry shows the change in chemical structure resulting from the hydrolysis of ester groups. The spectrum shows increasing peaks at 1001 cm^{-1} after an earlier decreasing period (Fig. 2) and a shift of peaks from 1040 to 1032 cm^{-1} over the course of the degradation (Fig. 3). The peaks at 1001 and at 1040 cm^{-1} represent the mono-substituted and the ortho-substituted aromatic rings, respectively. These peaks are usually strong in Raman and are normally expected to arise at 1000 ∓ 5 and 1033∓ 11 cm^{-1} bands, respectively [43]. Therefore, the observed decrease and shift may denote the modification of the initial structure (substituents sensitive bands) resulting from environmental attack followed by the production of alcohol structures that normally absorb between 1075 and 1000 cm^{-1} for aromatic secondary alcohol, and between 1036 and 970 cm^{-1} for axial cyclic secondary alcohol [43]. Figure 4 shows the gradual hydrolysis of ester groups that absorb at 1729 cm^{-1}. The peaks decrease according to an exponential law.

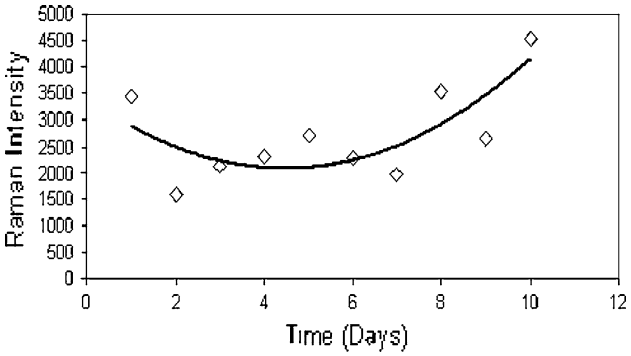

Fig. 2 Variation of Raman peaks at 1001 cm^{-1}

Moisture curve Figure 5 shows that the moisture percentage increases during degradation, denoting that the more the material structure is degraded the more the moisture penetrates inside the laminate. This explains the dramatic increase in absorbed moisture from the sixth day where the laminate has reached a high disintegration level corresponding to the lowest value of tensile strength recorded in Fig. 6. This shows that the moisture recorded inside the laminate is related to material disintegration from chemical attack and not due to Fickian diffusion. The curve shows an exponential trend corresponding to the suggested theoretical degradation model.

Post-curing effects The tensile strength was measured for samples subjected only to the temperature, for samples exposed to UV rays and temperature only, and for samples exposed to UV rays, temperature and chemical attack. Results are presented in Fig. 6. The plot shows that the laminate strength is not affected by the post-cure.

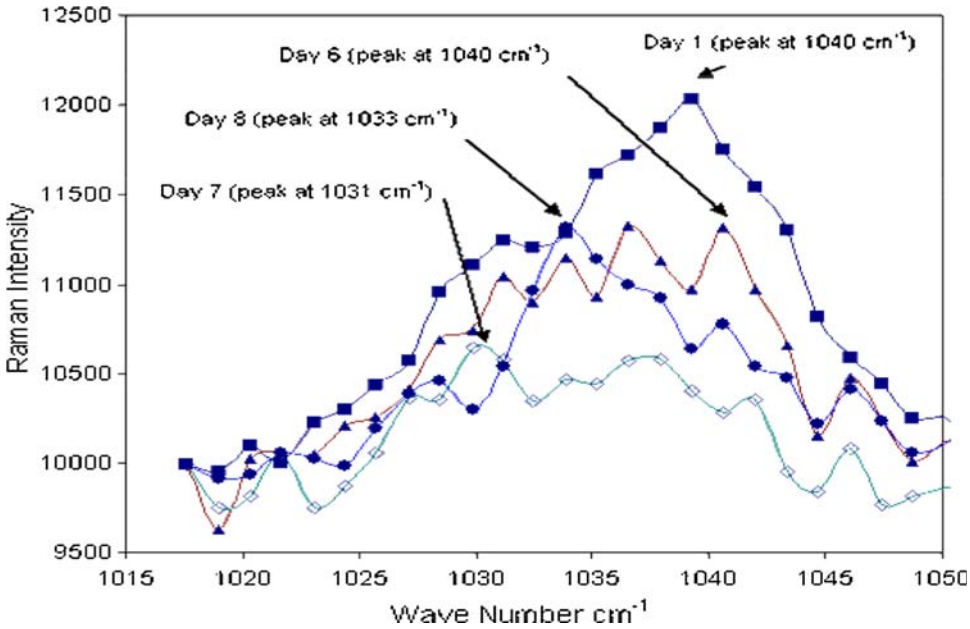

Fig. 3 Raman peaks shifting from 1040 to 1032 cm^{-1} during degradation

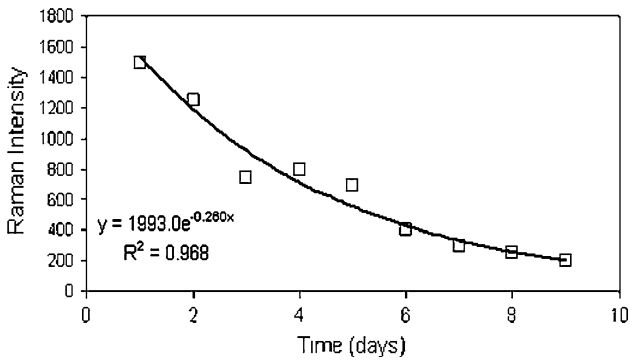

Fig. 4 Decrease of esters peaks (1729 cm^{-1}) during degradation

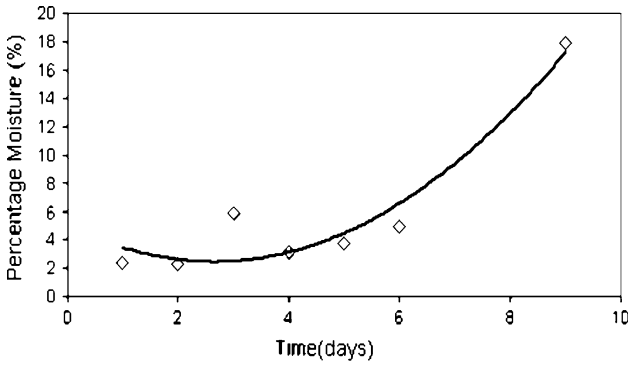

Fig. 5 Moisturization during degradation

Micrograph The Raman spectroscopy did not show any changes relative to glass fibre. SEM pictures, however, showed broken fibres following resin depletion (Fig. 7).

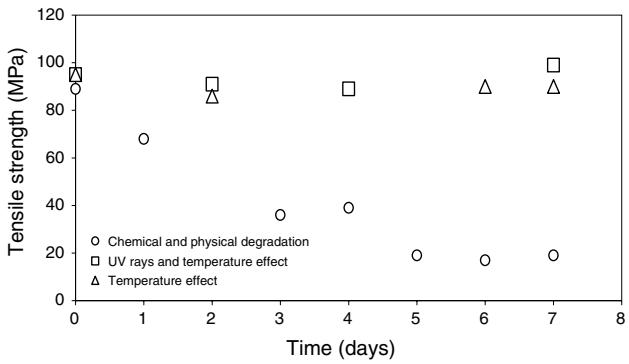

Fig. 6 Variation of tensile strength during degradation

Experiment 2: shear strength variation

Ten sets of 5 material samples were exposed to 10% sodium hydroxide aqueous solution for a maximum of 8 h at 80 °C. Sets were unloaded consecutively at 60 min intervals. Unloaded samples were immediately rinsed in abundant distilled water, in order to stop further reaction. Samples were then dried in desiccators for 24 h and then tested. Test results are presented in Fig. 8. The figure shows that the variation of shear strength resulting from the degradation follows an exponential trend.

Experiment 3: variation of storage modulus

The same procedure as for experiment 2 was followed with 10 sets of 3 samples of polyester composite laminates (see Table 1) over 9 h. The samples were then tested for shear modulus on an Anton Paar Physica MCR rheometer.

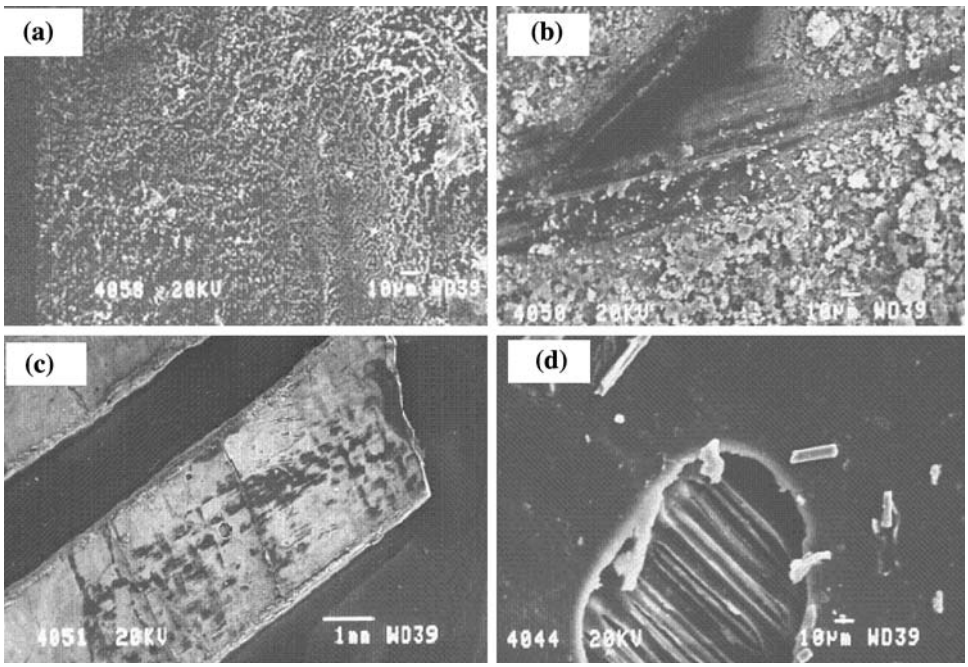

Fig 7 Micrograph of the specimen before and during the degradation **a** unexposed area, **b** progressive depletion of resin and fibre denudation, **c** exposed area showing pits and resin depletion, **d** inside of pits showing broken fibres

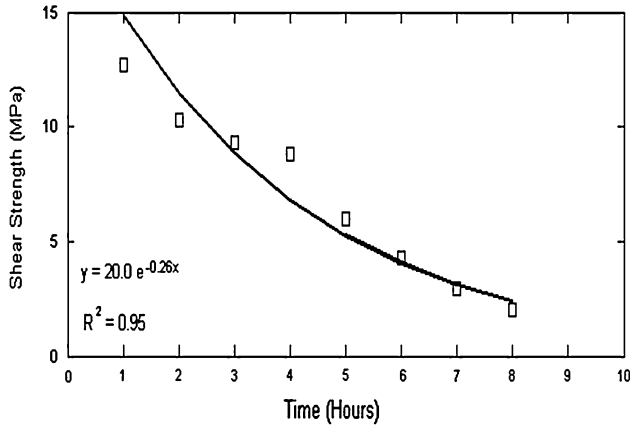

Fig. 8 Variation in shear strength due to chemical degradation

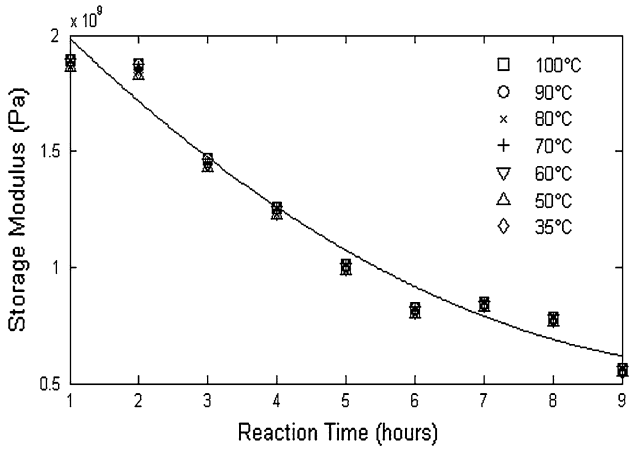

Fig. 9 Variation of storage modulus during degradation

Figure 9 presents the storage modulus variation for attacked samples at several temperatures below T_G.

Correlation between the model and experimental results

According to the model suggested in this analysis, in a constant environment the degradation of the material stiffness is linearly correlated to the variation in chemical link density and this variation rate is an exponential function of time. In order to experimentally assess the validity of this theoretical assertion, the degree of correlation between the index L_d and the material strength was numerically measured. Values of L_d were obtained from the Raman peaks of ester groups. The numerical regression of Raman peaks provided the degradation model (Figs. 4 and 10). The material strength was taken as the tensile strength (Table 3 and Fig. 6). The correlation coefficient R^2 is 0.97 (Fig. 11) indicating very good correlation between the model and experimental values.

The good linear correlation also provides the experimental verification of Eq. 6 showing a linear relationship between the material stiffness and the degree of chemical link degradation.

Comparing calculated and experimental material lifetimes based on tensile strength evolution

In order to perform the experimental comparison, the problem was set as follows: "What is the material lifetime if the minimal admissible value for its tensile strength is determined as a given percentage of the initial value?"

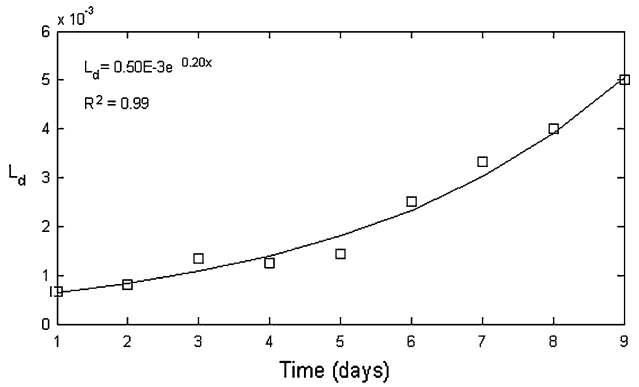

Fig. 10 Index of chemical links degradation deduced from ester groups reduction

From the degradation model of chemical structure in Fig. 4, the theoretical degradation rate for the material strength was determined by derivation:

$$\frac{dE_d}{dt} = -511.9e^{-0.2569t} \quad (44')$$

Based on Eq. 44′, the lifetimes were predicted for a range of different property retention values. The predicted values are compared to experimental values determined from Table 3. The comparison is presented in Fig. 12.

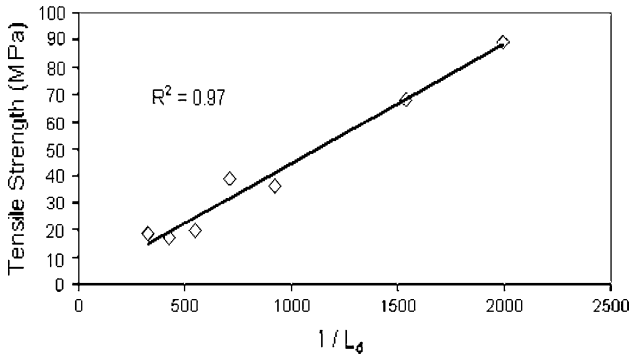

Fig. 11 Variation of tensile strength with chemical link density

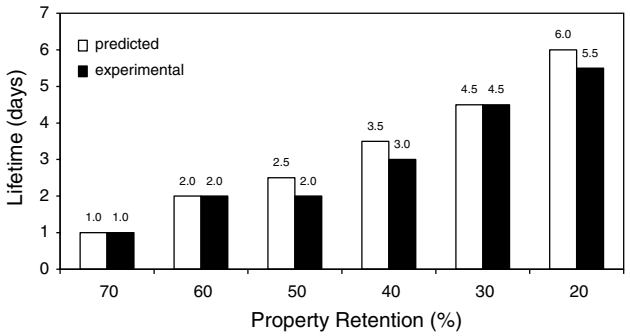

Fig. 12 Comparison of predicted and experimental lifetimes

Conclusions

Throughout the literature, the environmental degradation of FRP is described as a complex process. Modelling efforts are limited to partial models, most of the time empirical. No viable prediction method is yet available for the environmental degradation of the material mechanical strength. The analytical framework presented in this article relies on resolving the degradation process into only three components consisting of chemical degradation, physical degradation, and mechanical degradation. Based on material science theories, the analysis has demonstrated that, in a constant environment, the chemical and physical degradation of a polymeric matrix follows an exponential law. This results from the effect of the material rheology transformation on the diffusion process. The resulting mathematical model correlates the degradation rate directly to the material lifetime.

Experiments have been conducted using a range of measurement methods. These include Raman spectrometry for chemical structure changes, rheometry for storage modulus, and mechanical testing of tensile and shear strength evolution during degradation. All experiments confirm the validity of the suggested model. The degree of correlation between the model and the experimental process is very good.

The analysis also demonstrates that the chemical and physical degradation rate of a polymeric matrix is an ascending monotonic function of the environment. Consequently, the evaluation of environmental degradation in a laboratory can be conducted in a constant environment and laboratory test results can be directly translated to the real service environment. This is an important conclusion because many authors [1–3] have difficulty relating laboratory tests to actual service conditions.

Based on this mathematical model, a simple and practical prediction method has been suggested. The environmental degradation rate of a material in a real service environment can be determined in a laboratory based on tests conducted in a constant environment. This method requires monitoring only of the chemical structure change or any other material

Table 3 Experimental values of tensile strength

Duration (days)		0	1	2	3	4	5	6	7
Tensile strength (MPa)	AVG	89	68	–	36	39	19	17	19
	STD	0.019	0.001	–	0.008	0.000	0.002	0.003	0.002

property linearly correlated to the chemical structure. For the environmental conditions to be used in a laboratory, the method requires only the availability of statistical information such as the control chart of environmental variables including moisture, temperature, chemical concentration and UV ray intensity. Experiments conducted in a laboratory show that predicted degradation of the tensile strength of polyester fibreglass composite, based on this prediction method, is in good agreement with experimentally measured degradation.

The theoretical analysis presented in this article assumes that the material undergoing the physical and chemical degradation is not subject to any kind of mechanical load. Results obtained in this paper apply only to the case where mechanical stresses can be neglected. However, the suggested model provides a useful tool for assessing the chemical and physical degradation factors in cases involving both mechanical stress effects and physical and chemical degradation. This will be dealt with in a future paper.

Acknowledgements The author wishes to acknowledge the valuable support received from the University of the Witwatersrand, THRIP, DENEL and the DST/NRF Centre of Excellence in Strong Material (CoE-SM).

Appendix 1

Discrete integration of Eq. 14

Let Fig. 13 represent a laminate. According to pipe or tank model, the diffusion occurs in the direction perpendicular to the laminate. It is admitted that in the direction perpendicular to the diffusion, the material is homogeneous and therefore the diffusion coefficient is constant throughout a surface perpendicular to the diffusion direction.

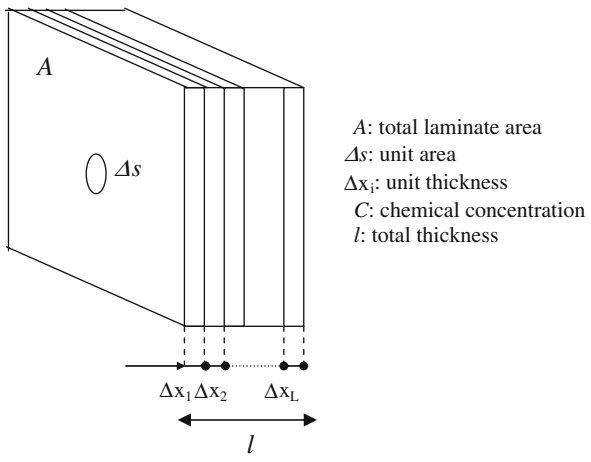

Fig. 13 Laminate portion

The flux of the diffused material through Δs is given as follows:

$$\Delta J_S = -D\frac{\Delta C}{\Delta x_i} \tag{45}$$

Assuming that the total area is made of n unit areas, the total flux through the area A is as follows:

$$\sum_{S=1}^{n} \Delta J_S = \sum_{S=1}^{n} \left(-D\frac{\Delta C}{\Delta x_i}\right)_S \tag{46}$$

As the diffusion coefficient is constant throughout A, the Eq. 46 may be written as follows:

$$\sum_{S=1}^{n} \Delta J_S = -nD\frac{\Delta C}{\Delta x_i} \tag{47}$$

The total flux through the laminate thickness l is given by the sum of the individual flux crossing each single surface layer as expressed below:

$$\sum_{i=0}^{l}\sum_{S=1}^{n} \Delta J_{S,i} = -nD\sum_{i=0}^{l}\frac{\Delta C}{\Delta x_i} \tag{48}$$

Now the sum of all the partial concentration gradients through the unit thickness Δx_i is equal to the total concentration gradient throughout the total thickness l:

$$\sum_{i=0}^{l}\frac{\Delta C}{\Delta x_i} = \frac{C_l - C_0}{l} \tag{49}$$

The total diffused material content in the laminate, at any instant, is exactly given by the total flux crossing the laminate at this instant. This flux is given by Eq. 48. Then taking into account Eq. 49:

$$C_{\text{ch}} = nD\frac{C_0 - C_l}{l} \tag{50}$$

In practice as $C_0 \gg C_l$, one can approximate the difference $C_0 - C_l$ to C_0.

$$C_{\text{ch}} = nD\frac{C_0}{l} \tag{51}$$

References

1. White JR, Turnbull SD (1994) J Mater Sci 29(3):584. doi: 10.1007/BF00445969
2. Barkatt A (2001) In: Jones RH (ed) Environmental effects on engineered materials. Marcel Dekker, New York, USA, p 419
3. Schutte CL (1994) Mater Sci Eng R 13:265
4. Springer GS (ed) (1981) Environmental effect on composite materials, vol 1. Technomic, Westport CT
5. Springer GS (ed) (1988) Environmental effect on composite materials, vol 3. Technomic, Westport CT
6. Avena A, Bunsell AR (1988) Compos 19(5):355
7. Srivastava VK (1999) Mater Sci Eng A 263:56

8. Tang JM, Springer GS (1988) In: Springer GS (ed) Environmental effect on composite materials, vol 3. Technomic, Westport CT, p 65
9. Mills NJ (1993) Environmental effects. In: Plastics, microstructure and engineering applications, 2nd edn. Edward Arnold, UK, pp 228
10. Springer GS (1988) In: Springer GS (ed) Environmental effect on composite materials, vol 3. Technomic, Westport CT
11. Chin JW, Ouadi K, Nguyen T (1997) J Compos Technol & Res JCTRER 19(4):205
12. Marsh LL, Lasky R, Seraphin DP, Springer GS (1988) In: Springer GS (ed) Environmental effect on composite materials, vol 3. Technomic, Westport CT, p 51
13. Liao K, Schultheisz C, Brinson C, Milkovich S (1995) Environmental durability of fiber-reinforced composites for infrastructure applications. In: Proceeding of the fourth ITI bridge. NDE users group conference, Absecon, NJ, USA
14. Lincoln Hawkins W (1972) In: Lincoln Hawkins W (ed) Polymer stabilization. Wiley-Interscience, NY, p 1
15. Kirkaldy JS, Young DJ (1981) Diffusion in the condensed state. Institute of Metals, London, pp 1, 310
16. Thominet F, Bellenger V, Merdas I, Launay A, Gauthier L, Salmon L (1997) Compos Sci Technol 57:1119
17. Rao RMVGK, Balasubramania N, Chanda M (1988) In: Springer GS ed. Environmental effect on composite materials, vol 3. Technomic, Westport CT
18. Sonawala SP, Spontak RJ (1996) J Compos Mater 31(18):4745
19. Maron GA, Broutman LJ (1981) Polym Compos 2(3):132
20. Stone MA, Schwartz IF, Chandler HD (1997) Compos Sci Technol 57:47
21. MacCallum JR (1989) In: Eastmond GC, Ledwith A, Russo S, Sigwalt P (eds) Comprehensive polymer science, V6 polymer reactions. Pergamon Press, UK, p 529
22. Kaczmarek H (1996) Polym 37(2):189
23. Sookay NK, Von Klemperer CJ, Verijenko VE (2003) Compos Struct 62:429
24. Startsev OV, Krotov AS, Startseva LT (1999) Polym Degrad Stab 63:183
25. Lee B-S, Motoyama T, Ichikawa K, Tabata Y, Lee D-C (1999) Polym Degrad Stab 66:271
26. Prian L, Barkatt A (1999) J Mater Sci 34:3977. doi:10.1023/A:1004647511910
27. Kumar BG, Singh RP, Nakamura T (2002) J Compos Mater 36(24):2713
28. Ciriscioli PR, Lee WI, Peterson DG, Springer GS, Tang JM (1988) In: Springer GS (ed) Environmental effect on composite materials, vol 3. Technomic, Westport CT, p 45
29. Pritchard G, Speake SD (1987) Compos 18(3):227
30. Nakamura T, Singh RP, Vaddadi P (2006) Exp Mech 36:257
31. Reich L Stivala S (1971) Element of polymer degradation. McGrawHill, New York, pp 1, 165, 229
32. Verdu S, Verdu J (1997) Macromol 30:2262
33. Belan F, Bellenger V, Mortaigne B, Verdu J (1997) Polym Degrad Stab 56:301
34. Sevostianov I, Sookay NK, Von Klemperer CJ, Verijenko VE (2003) Compos Struct 62:417
35. Celina M, Gillen KT, Assink RA (2005) Polym Degrad Stab 90:395
36. SASOL (2002) Code of practice for inspection of in-service non-metallic equipments. Specification SP-100-42-2A Revision 1. SASOL, South Africa
37. ISO 3417–1977(E) (1984) Measurement of vulcanization characteristics with the oscillating disc curemeter. Rubber—mixes and vulcanized rubber ISO standards handbook 22, vol 2. ISO, Switzerland, p 225
38. Ravve A (1967) Organic chemistry of macromolecules: an introductory textbook. E. Arnold, London, p 48
39. Lenz RW (1967) Viscoelastic behavior. Organic chemistry of synthetic high polymers. Interscience, NewYork, p 31
40. McCrum NG, Buckley CP, Bucknal CB (1997) Principles of polymer engineering. Oxford University Press, Oxford
41. Goodwin JW, Hughes RW (2000) Rheology for chemists an introduction. The royal society of chemists. Great Britain, Cambridge
42. Bondi A (1956) In: Eirich FR (ed) Rheology theory and application, vol 1. Academic Press Inc., New York, p 321
43. Colthup NB, Daly LH, Wiberly SE (1975) Introduction to infrared and Raman spectroscopy, 2nd edn. Academic Press, New York, p 257